Carbonate characterization, property simulation and upscaling using microtomography

Jie Liu* (University of Western Australia, Australia), Reem Freij-Ayoub (CESRE, CSIRO), Gerald G. Pereira (CMIS, CSIRO), Ben Clennell (CESRE, CSIRO), Klaus Regenauer-Lieb (University of Western Australia)

Abstract

We characterise a microstructure by its volume fraction, the specific surface area, the connectivity (percolation) and the anisotropy of the micro-structure. Petro-physical properties (permeability and mechanical parameters) are numerically simulated based on representative volume elements (RVEs) from microstructural models. The validity of the results from these forward simulations is dependent on selecting the correct size of the RVE. We use stochastic analysis of the microstructures to deter-mine the size of a geometrical RVE, and upper/lower bound finite element computations on a series of models with different sizes to determine a mechanical RVE. Upscaling of properties is achieved by means of percolation theory. We detect the percolation thres-hold by using a shrinking/expanding algorithm on our static micro-CT images of rocks. Parameters of the scaling laws can be extracted from quantitative analyses and/or numerical simulations on the original micro-CT images and the derivative models created by shrinking/expanding the pore-structure. Scaling laws describe how properties which are obtained at the micro-scale can be used effectively on larger scales. Five samples of microtomography of carbon-ate are analyzed using this workflow. Individual and common characteristics are obtained.

1 Introduction

Carbonate reservoirs offshore Brazil have a great poten-tial as a source of oil and gas. Their variable lithofacies and diagenetic history make their characterization espe-cially challenging. The first major objective of this study is to characterise carbonate structures and investigate the relationship between porosity and permeability.

Coupled geomechanical modeling is needed at the stages of planning, drilling and production of a hydrocarbon field. Various types of modeling require input parameters that need to be evaluated using multi-scale laboratory experiments and various upscaling techniques. The second major objective of this study is to determine the geomechanical properties of carbonates across a range of scales.

Microtomography enables the detection of internal structure of rocks on micro- to nano-scales and opens a new way to quantify the relationship between the microstructure and their mechanical and transport properties. Numerical computations of microtomographic data have shown good agreement with experimental data for fluid flow and elastic properties [1, 2]. However, the extension of the methodology to plastic properties is still a poorly understood area. Owing to the finite size of microtomographic images, the higher the resolution, the smaller the length scale of the sample that is contained in a certain number of pixels or voxels. This leads to the immediate challenge to detect the internal structure of rocks across micro to nano scales and at the same time connect the images to the macro-scale essential for describing the reservoir.

In this study, we use microtomography of carbonate to characterise the microstructures and simulate the permeability of different structures. We also analyze the mechanical response and focus on plastic strength at micro-scale of the samples. Then we use percolation theory to conduct upscaling of rock properties from microtomography.

2 Strategy and methodology

We have developed a strategy and workflow of microtomographic analyses, see Figure 1. Our work starts from the gray scale images of microtomography and involves three main components based on the binary data obtained after image segmentation. The binary data have only two phases -- pores and solid, being represented by 0 and 1, respectively. Three main components in the workflow are:

1) Geometrical analysis. It conducts quantitative analysis, including stochastic analysis, of the geometry of the pores. General parameters such as porosity, connectivity, specific surface area, and the fractal dimension are obtained. Stochastic analysis outputs probabilities of porosity, percolation, and anisotropy of different model sizes [3]. The size of a representative volume element (RVE) can be determined when the probabilities converge with an increase of the model size being analyzed. Permeability of rock is directly related to the geometry of pores, thus the geometrical RVE is suitable for computing permeability.

2) Mechanical analysis. In this component we determine the size of mechanical RVE by detecting the mechanical responses of maximum and minimum (upper and lower bounds) entropy productions of models of different sizes [4, 5]. Then the plastic response of the microstructural model is analyzed over the mechanical RVE.

3) Extracting critical exponents of key parameters of rock property. Here we use a shrinking/expanding algorithm [6] to create a series of derivative models with different volume fraction. Based on percolation theory, parameters

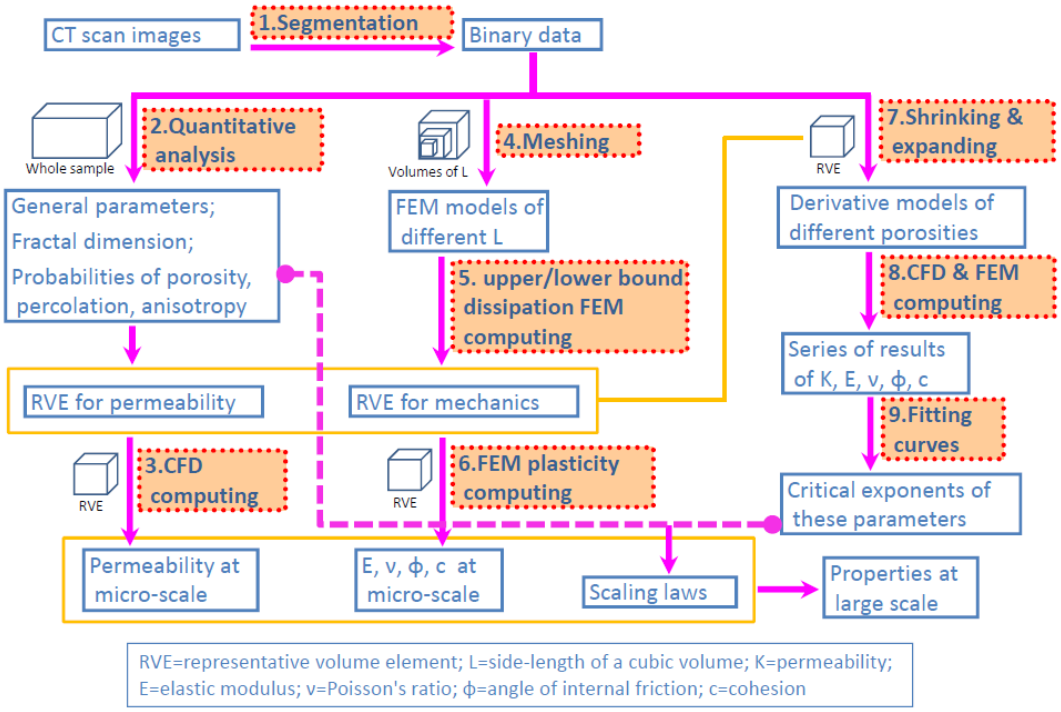

Figure 1: Workflow for upscaling of rock properties from microtomography

such as permeability, elastic modulus, and yield stress change exponentially when the porosity approaches the percolation threshold. They have the form $K = (p - p_c)^{\chi}$, $E = (p - p_c)^{f}$, $\sigma_y = (p - p_c)^{T_f}$, where K, E and σ_y are permeability, elastic modulus and yield stress, respectively, p is the volume fraction and p_c is the percolation threshold [7 - 10]. The exponential indices χ, f or T_f, describing this scaling tendency are called critical exponents.

With any two critical exponents and/or the fractal dimension, scaling laws are defined. Scaling laws, the percolation threshold, and some other parameters such as the crossover length are constraints used for upscaling properties from micro-scale to large scale.

3 Results

We analyzed five samples running all the procedures described in Figure 1. These five samples are different from each other even at a glance of the microtomographic images. Thus the characteristics can be very different; however, there are also some common features. In the following, one sample is illustrated as an example. A summary of characteristics or results of these five samples is given briefly as well.

A typical slice of microtomographic images of one of the samples (CP10) is shown in Figure 2a. We crop a rectangular volume of 1000^3 and segment the volume to binary data. The cropped and segmented slice is shown in Figure 2b. The pore-structure in 3D is shown in Figure 2c. The resolution of this sample is 1.85 μm.

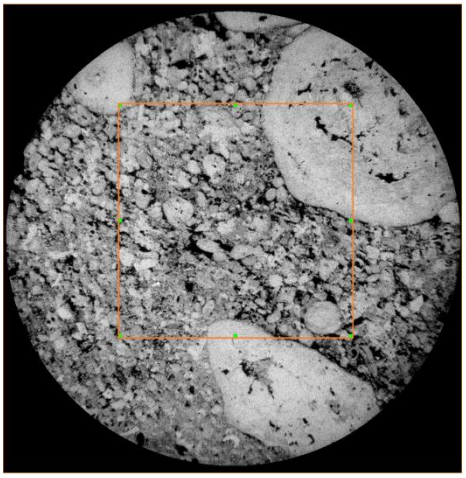

(a)

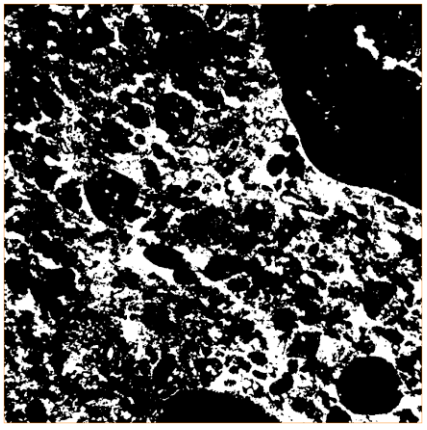

(b)

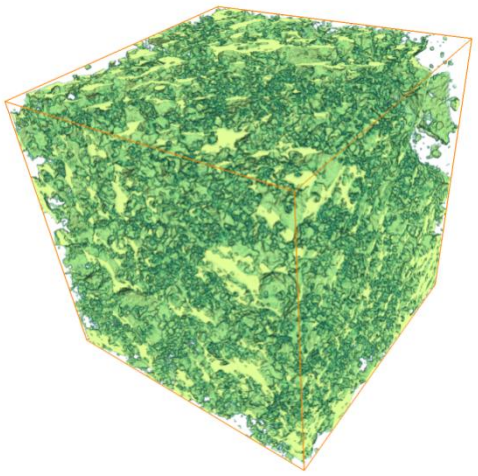

(c)

Figure 2: A slice of microtomographic images (a); segmented portion of the slice; and pore-structure in 3D (c).

3.1 Geometrical analysis

The porosity of this sample is 26.1% calaculated from the microtomographic images. Our analyses show that there is an inter-connected pore-structure which constitutes 96% of the pore volume. There are more than 86,000 isolated pores (with closed surface) occupying 4% pore space, and these pores do not affect the fluid flow. The percolating pore-structure is almost isotropic in three directions. The specific surface area is 0.0725 μm^{-1}, which is quite high comparing with the other four samples meaning pores are tortuous and surfaces are rough.

Scale dependent characteristics are obtained by means of stochastic analysis, in particular, using the moving window method [3]. Moving window sizes of various side-length are analyzed, with L = 50, 100, 150, 200, 250, 300, 350, 400, 450 voxels. Probabilities of porosity, percolation, and anisotropy are shown in Figure 3. As we can see from all these 4 diagrams, curves of L = 350, 400, and 450 voxels are close to each other and so these curves are considered convergent. We conclude that the size of geometrical representative volume element (RVE) for this sample can be 400^3. However, we should be aware of the uncertainty (or the range) of the porosity and isotropy index of the geometrical RVE.

The Lattice-Boltzmann method is used to simulate the pore-scale fluid flow within the RVE. From the calculated steady state flow field we obtain a permeability of 0.59 Darcy for this sample.

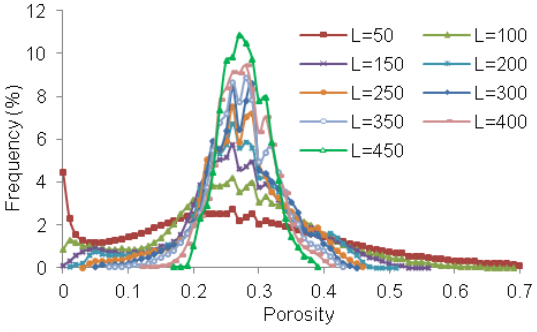

(a)

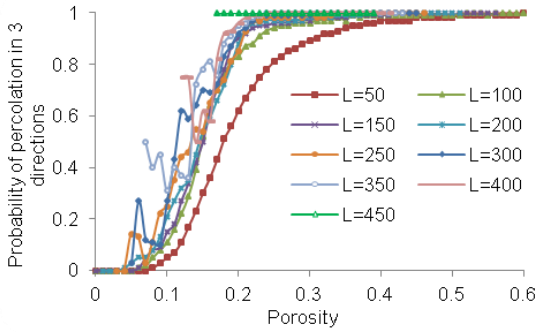

(b)

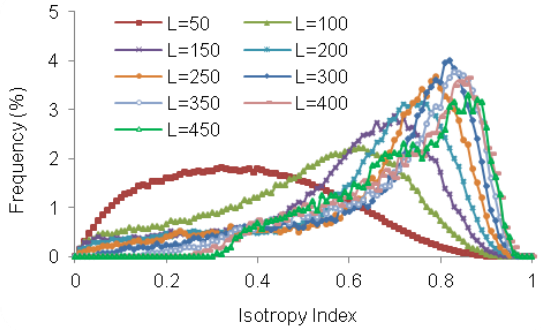

(c)

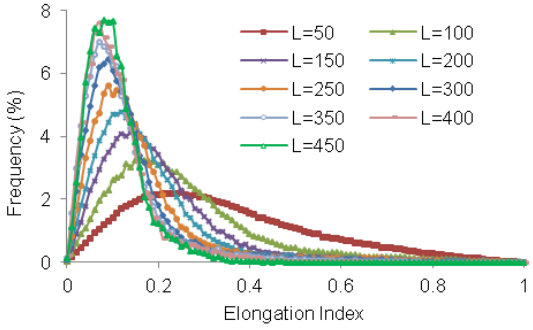

(d)

Figure 3: Scale-dependent characteristics from stochastic analyses. (a) Probability of porosity; (b) probability of percolation; (c) probability of isotropy index; (d) probability of elongation index.

Summary of the five samples: The five samples have different microstructural characteristics, e.g., porosity ranges from 15% to 26%, while specific surface area changes from 0.017 to 0.075 μm^{-1}. The convergence of stochastic analyses shows different uncertainties while more generally gives the size of RVE 350^3 to 500^3 voxels. For some other samples within this study, the size of a geometrical RVE is not determined as curves are not convergent. In this situation, an arbitrarily selected volume of around 400^3 is used for CFD simulations as a case study. Simulated permeability is in the range of 0.05 – 0.66 Darcy.

3.2 Mechanical analyses

We use the thermodynamic upper and lower bound principles postulated by Regenauer-Lieb et al. [4, 5] to quantify whether our computations of the mechanical response of models with different sizes have converged such that they can deliver homogenized values.

Eight cubic volumes of side-length L = 40 to 300 are analysed. Figure 4 displays the upper and lower bounds

of the elastic modulus and shear modulus for different volume sizes. Convergence can be seen for the volume with L larger than 200. Thus, the mechanical RVE is determined as 200^3 voxels for this carbonate sample.

We use the linear Drucker-Prager plasticity and finite element method to simulate the rock failure of a mechanical RVE. To determine cohesion and the angle of friction, the relationship $\sigma_y = \sigma_n \tan\varphi + c$ is used, where σ_y and σ_n are yield stress and normal stress computed from Drucker-Prager plasticity, c and φ are cohesion and the angle of internal friction of the rock. To deduce c and φ two sets of σ_y and σ_n results are required from the model. Thus two cases giving different pressure (or normal stress) conditions will be simulated, and two different yield stresses are expected.

We only considered elastic-perfect plasticity and impose a displacement load on the top surface in the z direction. Two cases of experimental conditions are simulated: Case 1 is an unconfined compression and Case 2 is a uniaxial strain condition. Stress-strain curves (Figure 5) show that Case 1 performs elastic-perfect plasticity and Case 2 performs plastic hardening. Plotting the volume average of mean stress versus von Mises stress of the model (Figure 6) for Case 1 and Case 2, we obtained a model cohesion of 21 MPa and a friction angle of 7.6°.

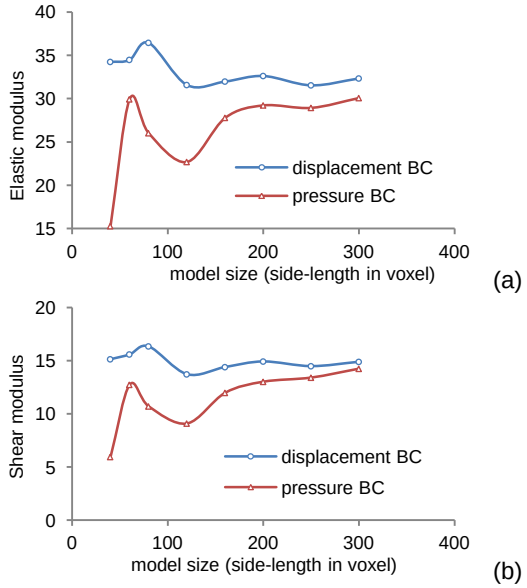

Figure 4: Elastic and shear moduli change with model-size L for upper and lower bounds.

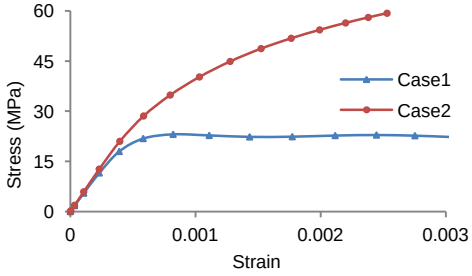

Figure 5: Stress-strain relationships of Case1 and Case2 plastic computations.

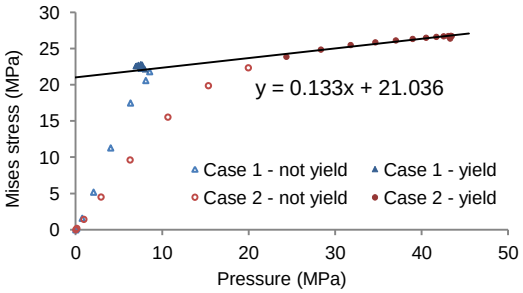

Figure 6: Fitting cohesion and friction angle from Case1 and Case2.

Summary of the five samples: The sizes of the mechanical RVE of these five samples are between 200^3 to 300^3, meaning that the mechanical RVE is smaller than the geometrical RVE size for each of those samples. As expected, it is found that the yield stress of the porous carbonate is (relatively) higher when the porosity is lower from the five samples with porosity from 15% to 26%. Cohesion and friction angle have the same trend. Both yield stress and cohesion are in a narrow range from 20.5 MPa to 23 MPa when the yield stress of intact solid is assumed to be 30 MPa in this study. Values of the friction angle, however, show more variation as they fall in the angle from 7.6° to 21.5° for these five samples, when the friction angle of intact solid is assumed to be 40°. Moreover, models of similar porosities may have quite different friction angles, suggesting that the friction angle is related to the microstructures as well.

3.3 Critical exponents

The critical exponents of permeability and yield stress are extracted in this study based on the relationships $K = (p - p_c)^X$ and $\sigma_y = (p - p_c)^{T_f}$. With a series of models at different volume fraction p and the corresponding permeability or yield stress, the critical exponent can be fitted. To do this, the percolation threshold should also be known. A shrinking/expanding algorithm [6] is used to create a series of derivative models with different volume fractions. Then the percolation threshold can be determined from the volume fraction of the critical model. The critical model is the derivative model that is with the smallest percolating cluster. Permeability and yield stress are simulated on the derivative models that are close to the critical model to make the approach work.

To detect the critical exponent of permeability, we shrank the pore-structure and found the percolation threshold of pores to be 4.86%. Five derivative models with porosity from 5.49% to 13.57% which are close to the percolation threshold were simulated using the Lattice-Boltzmann method and permeability values were obtained (see Table 1). By fitting the difference of porosity and the percolation threshold $|p - p_c|$ versus permeability in log-log plot, we found the critical exponent of permeability to be 0.67.

To detect the critical exponent of yield stress, we shrank the solid-structure (or expanded the pore-structure). After 10 shrinking steps, the model is percolating only in the y direction and its volume fraction, 7.57%, is recognized as the percolation threshold of solid. Five derivative models

close to the percolation threshold with solid volume fractions from 12.79% to 21.25% were analyzed and their yield stresses were obtained. By fitting the yield stress versus the difference between the volume fraction and the percolation threshold $|p - p_c|$ in log-log plot (see Fig. 7), we obtained the critical exponent of yield stress to be 2.3.

Table 1: Porosity of derivative models and the permeability from Lattice-Boltzmann simulations

Parameter	model1	model2	model3	model4	model5
φ (or p)	0.055	0.076	0.087	0.119	0.136
K in x (D)	0.067	0.101	0.119	0.183	0.220
K in y (D)	0.058	0.089	0.104	0.158	0.189
K in z (D)		0.094	0.111	0.169	0.202
K (ave, D)	0.063	0.095	0.111	0.170	0.204

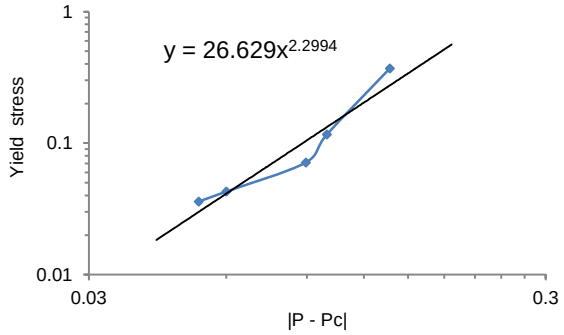

Figure 7: Fitting the critical exponent of yield stress

Summary of the five samples: The critical exponent of permeability is close to each other for the five samples we analysed. The value is around 0.66. which is smaller than the theretical result of 2.0 that was derived from analyses of random models [10]. The critical exponent of yield stress, however, is in the range of 0.65 to 2.3 for different microstructures and different loading cases. An estimation from random model is 2.58 to 2.76, which was based on theretical derivations and a few laboratory experiments [10]. Our results indicate these natural samples are more complicated than the theoretical random models.

Conclusions

We have established a strategy and workflow of microtomographic analyses for 1) the characterization of microstructures, 2) the determination of the sizes of geometrical and mechanical RVEs, 3) the forward simulations of permeability and mechanical parameters on RVEs, and 4) the extraction of critical exponents and the upscaling of the properties of rock using percolation theory.

Five carbonate samples were analyzed in this study using the workflow. Individual characteristics and common features were found from the analysis. The relationships of microstructures with permeability and/or mechanical parameters were detected. The critical exponents are basic elements of scaling laws describing the scale dependent characteristics of some petrophysical parameters. Our results show that natural samples are far more complex than theoretical random models. Our workflow allows the investigator to obtain results from real rock data. This analysis can therefore provide more practical information than previous theoretical models. We propose this workflow as a new method for assessing scaling relationships from micro-scale to reservoir scale for drilling and production of hydrocarbon fields.

Acknowledgments

We thank Petrobras' support for this research. We are grateful to iVEC for technical support and access to its visualization facilities and supercomputers. Claudio Delle Piane and Valeriya Shulakova in CESRE contributed to data acquirement and image pre-processing of micro-tomography. We thank Ali Karrech, and Thomas Poulet in CESRE for their help on finite element computing and pre-/post- processing.

References

[1] C.H. Arns, M.A. Knackstedt, W.V. Pinczewski, W.B. Lindquist: Accurate estimation of transport properties from microtomographic images. *Geophysical Research Letters*, 28 (2001), 3361-3364.

[2] M.A. Knackstedt, C.H. Arns, M. Saadatfar, et al.: Elastic and transport properties of cellular solids derived from three-dimensional tomographic images. *Proc. R. Soc. A*, 462 (2006): 2833-2862

[3] J. Liu, K. Regenauer-Lieb, C. Hines, et al.: Improved estimates of percolation and anisotropic permeability from 3-D X-ray microtomographic model using stochastic analyses and visualization. *Geochem., Geophys. Geosyst.*, 10 (2009), Q05010, doi: 10.1029/2008GC002358.

[4] K. Regenauer-Lieb, A. Karrech, H.T. Chua, et al.: Non-equilibrium Thermodynamics for multi-scale THMC coupling. *GeoProc2011*, Perth, 6-9 July 2011.

[5] K. Regenauer-Lieb, A. Karrech, H. Chua, F. Horowitz, and D. Yuen: Time-dependent, irreversible entropy production and geodynamics. *Philosophical Transactions of the Royal Society London, A,* 368(2010), 285-300.

[6] J. Liu, K. Regenauer-Lieb: Application of percolation theory to microtomography of structured media: percolation threshold, critical exponents and upscaling, *Physical Review E*, 83 (2011), 016106, doi: 10.1103/ PhysRevE.83.016106.

[7] D. Stauffer, A. Aharony: Introduction to percolation theory (Second ed.). Taylor & Francis Ltd., London, 1994.

[8] K. Sieradzki and R. Li: Fracture behavior of a solid with random porosity. *Physical Review Letters*, 56(1986): 2509 – 2512.

[9] L. Benguigui, P. Ron, and D. J. Bergman: Strain and stress at the fracture of percolative media. *J. Physique*, 48(1987): 1547-1551.

[10] M. Sahimi: Non-linear and non-local transport processes in heterogeneous media: from long-range correlated percolation to fracture and materials breakdown. *Physics Reports*, 306(1998): 213-395.